Original Paper

Non-Gaussian Nature of the SDOF Response to Gaussian Vehicle Vibrations

Akira HOSOYAMA*, Kazuki TSUDA*, and Shogo HORIGUCHI*

This study aims to verify the equivalence between a Gaussian random vibration extracted from a vehicle vibration and that generated by a current vibration controller. The equivalence was evaluated by calculating the kurtosis from a single degree of freedom (SDOF) response, assuming that an SDOF system serves as the packaged product. Depending on the natural frequency of the packaged product, the SDOF response to the Gaussian random vibration generated by the current vibration controller was found to be a Gaussian random vibration, while the SDOF response to the Gaussian random vibration extracted from the vehicle vibration, a non-Gaussian random vibration. The results demonstrate that both the Gaussian random vibrations may not be equivalent. Further, solely the power spectrum density (PSD) and probability density function (PDF) are not sufficient to completely understand the nature of the vibrations; the PDFs of the SDOF responses also need to be considered.

Keywords: random vibration; Gaussian distribution; SDOF; vibration testing; kurtosis response spectrum

1 Introduction

In recent years, the global e-commerce market has expanded and the number of delivery parcels has increased. As a result, the number of transportation accidents that are attributed to vibrations has increased. In addition, the importance of vibration testing, which is performed to confirm the safety of the packaged products against vibrations, is also increasing. Current vibration test standards[1)2)3)] recommend using a vertical Gaussian random vibration test. However, it has been demonstrated that during transportation, non-Gaussian random vibrations often occur. Thus, a gap arises between the vibration environment that is reproduced by the vibration controller and the actual vibration environment.[4)5)] This gap can lead to transportation accidents, even if the packaged products meet the vibration test requirements. Therefore, it is necessary to improve the accuracy of vibration testing.

Several studies have been performed on non-Gaussian random vibration generation methods[6)] to reproduce the non-Gaussian nature of the actual vibration environment. In this regard, the polynomial transformation, phase control, and random Gaussian sequence decomposition methods have been proposed as representative non-Gaussian random vibration generation methods.

The polynomial transformation method is used to convert the Gaussian random vibrations into stationary non-Gaussian random vibrations by using a polynomial function. [7)8)] This method is easy to use for simulating the non-Gaussian random vibrations; however, it has been demonstrated that the power spectral density (PSD) is distorted during the conversion. [9)]

In contrast, the phase control method is used to generate stationary non-Gaussian random vibrations by controlling the Fourier phase. Steinwolf[10)] proposed a method to control the Fourier phase by using a mathematical formula that relates the Fourier phase to kurtosis. The authors[11)] proposed a method of generating non-Gaussian random vibrations by incorporating the concept of a seismic wave simulation, in

* Osaka Research Institute of Industrial Science and Technology, 2-7-1, Ayumino, Izumi-city, Osaka 594-1157, Japan
Corresponding author: Akira Hosoyama. Tel:0725-51-2703, Fax:0725-51-2639, E-mail: hosoyama@tri-osaka.jp

which the shape of a seismic wave is controlled by the Fourier phase. The phase control method does not cause any distortion in the PSD in principle because the kurtosis is controlled by the Fourier phase.

Finally, the random Gaussian sequence decomposition method is used to generate non-stationary non-Gaussian random vibrations. This is achieved by decomposing the non-Gaussian random vibrations into Gaussian segments with different amplitudes. The random Gaussian sequence decomposition method is based on the hypothesis that the peakedness of the vehicle vibration is due to the non-stationarity of the vehicle vibration caused by the changes in the vehicle speed and road surface roughness. An advantage of this method is that it can reproduce the non-stationarity vibration.

Many studies have focused on the random Gaussian sequence decomposition in the domain of packaging. Rouillard et al.[12] proposed a method to decompose the non-Gaussian random vibrations into Gaussian segments with different amplitudes and generate non-Gaussian random vibrations as the sum of these Gaussian segments. Griffiths et al. [13] proposed a method to decompose the non-Gaussian random vibrations into Gaussian segments through an iterative process that uses the discrete wavelet transformation. Zhou et al. [14] proposed another method for a similar decomposition by detecting shocks that use a moving crest factor, while Bonnin et al. [15] suggested an iterative process that uses the sum of the weighted Gaussians. Thus, several decomposition methods for the non-Gaussian random vibrations have been proposed, which contributes to improving the accuracy of vibration testing and they enable us to reproduce a vibration environment that is close to the actual transportation.

On the other hand, the random Gaussian sequence decomposition method assumes that the Gaussian random vibrations that are derived using an actual vehicle and those that are derived using a vibration controller are equivalent. However, the equivalence between both these vibrations has not been sufficiently verified thus far. Since the equivalence between these vibrations is the basis of the random Gaussian sequence decomposition method, the verification of the equivalence is crucial.

In this study, the vehicle vibration is measured using a small van and is decomposed into several Gaussian random vibrations. In addition, the Gaussian random vibration is generated based on the PSD obtained from the decomposed data. Furthermore, the equivalence between the two types of Gaussian random vibrations was evaluated by calculating the kurtosis from a single degree of freedom (SDOF) response, assuming that an SDOF system serves as the packaged product.

2 Gaussian vehicle vibration and Gaussian shaker simulation

2.1 Gaussian vehicle vibration

The vertical acceleration that is exhibited by the vehicle bed of a small van (Fig. 1) traveling on a local road in Japan was measured with an acceleration sensor (type 4326A, Brüel & Kjær, Denmark) that was installed on the vehicle bed, as illustrated in Fig. 2. The details of the vehicle specifications and the measurement conditions are presented in Tables 1 and 2, respectively. Fig. 3 depicts the acceleration data that was measured on the vehicle bed, which also includes the data that was measured at sections where the vehicle stopped at a traffic signal. To extract the running sections, the sections where the acceleration root mean square (RMS) was less than 0.4 m/s^2 for 1 s (1280 points) were removed, and the remaining sections were connected to remove the stopping sections. Figs. 4 and 5 depict the zero-set data when the sections had an acceleration RMS of less than 0.4 m/s^2, along with the data for these removed sections, respectively. Table 3 presents the acceleration RMS and the kurtosis values of the acceleration data that is depicted in Fig. 5. Here, a kurtosis is a measure that represents the characteristics of a non-Gaussian distribution. Kurtosis K can be expressed as follows:

$$K = \frac{\frac{1}{N}\sum_{i=1}^{N}((x_i - x_m)^4)}{\left(\frac{1}{N}\sum_{i=1}^{N}(x_i - x_m)^2\right)^2} \tag{1}$$

where N is the number of data points, x_i is an acceleration value, and x_m is the average of acceleration values. A Gaussian distribution has a kurtosis of 3. A kurtosis greater than 3 indicates that the distribution peaks more and has heavier tails than a Gaussian distribution.

Fig. 1 Test vehicle used in this study

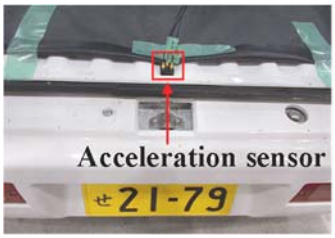

Fig. 2 Acceleration sensor installed on the vehicle bed

Table 1 Vehicle specifications

Vehicle type	Small van (Daihatsu HIJET)
Total vehicle weight	1380 kg
Tread (front)	1305 mm
Tread (rear)	1300 mm
Wheelbase	2450 mm

Table 2 Measurement conditions

Road type	Suburban road
Travel distance	10 km
Speed	0–60 km/h
Sampling rate	1280 Hz
Sampling size	1024
Measuring direction	Vertical
Acceleration sensor position	Rear end of vehicle bed (Fig. 2)

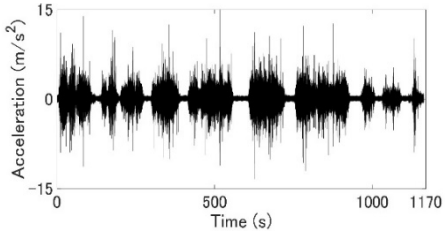

Fig. 3 Acceleration data measured on the vehicle bed

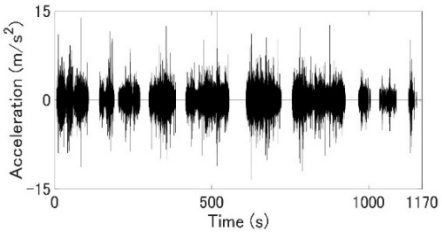

Fig. 4 Zero-set data for the sections where the acceleration RMS is less than 0.4 m/s^2

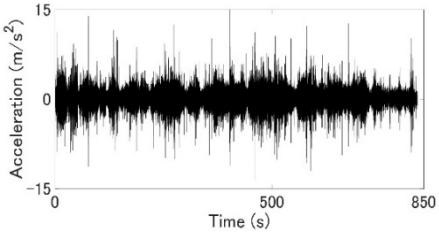

Fig. 5 Acceleration data after removing the sections that have an acceleration RMS that is less than 0.4 m/s^2

Table 3 Acceleration RMS and the kurtosis of the acceleration data that is shown in Fig. 5

Acceleration RMS (m/s^2)	Kurtosis
1.3	8.2

The acceleration data in Fig. 5 are classified by the conditions of the acceleration RMS that are listed in Table 4 and it is decomposed into seven types of vibrations. Fig. 6 depicts the vibrations that are extracted by the conditions of the acceleration RMS in Table 4 and the connected vibrations. Table 5 presents the acceleration RMS and kurtosis for the seven types of decomposed vibrations. In Table 5, the kurtosis of "Vibration 3" is 3.1, which is the closest value to three among the seven types of vibrations. Therefore, in this study, "Vibration 3" is used as the Gaussian random vibration obtained from an actual vehicle.

Table 4 Decomposed conditions of the acceleration data that is shown in Fig. 5

	One-second RMS, a (m/s^2)
Vibration 1	$0.4 \leqq a < 0.6$
Vibration 2	$0.6 \leqq a < 0.8$
Vibration 3	$0.8 \leqq a < 1.0$
Vibration 4	$1.0 \leqq a < 1.5$
Vibration 5	$1.5 \leqq a < 2.0$
Vibration 6	$2.0 \leqq a < 3.0$
Vibration 7	$3.0 \leqq a$

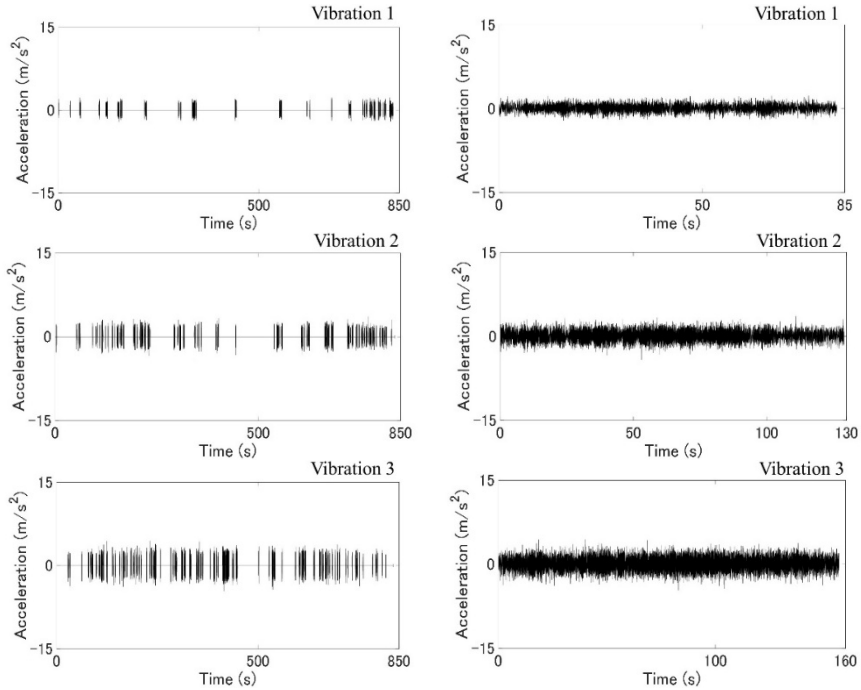

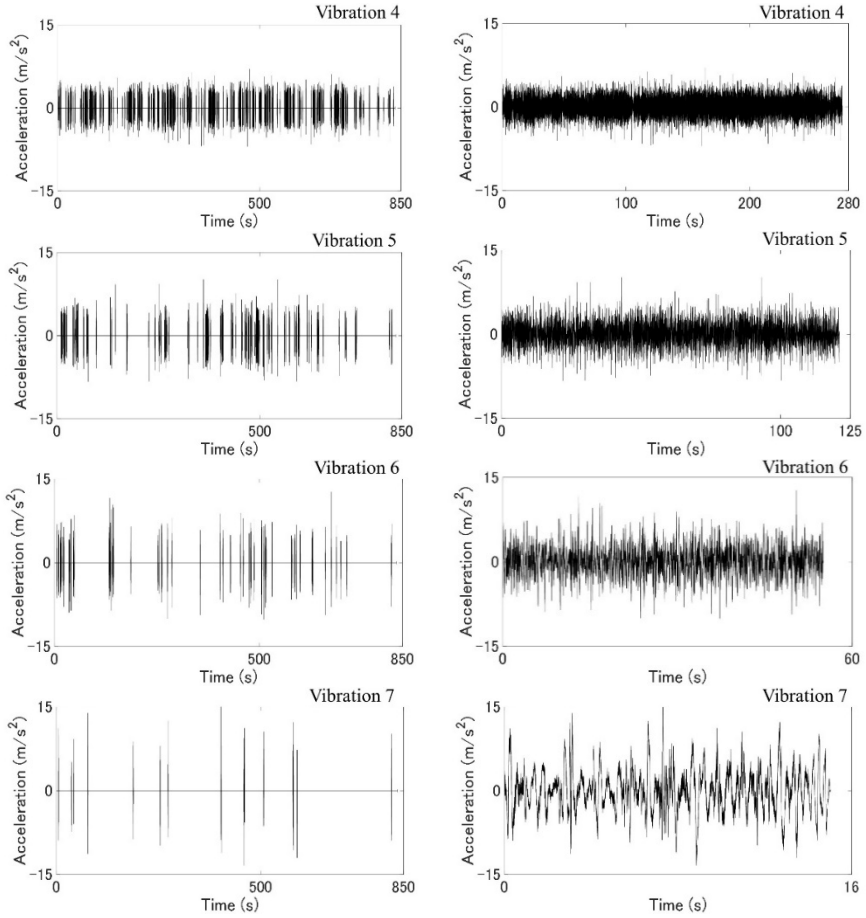

(a) Extracted data (b) Connected data

Fig. 6 Gaussian decomposition of the acceleration data that is shown in Fig. 5

Table 5 Acceleration RMS and the kurtosis of the decomposed vibrations that are shown in Fig. 6

	Acceleration RMS (m/s^2)	Kurtosis
Vibration 1	0.5	3.2
Vibration 2	0.7	3.2
Vibration 3	0.9	3.1
Vibration 4	1.2	3.5
Vibration 5	1.7	3.6
Vibration 6	2.3	3.6
Vibration 7	3.7	3.5

2.2 Gaussian shaker simulation

The Gaussian random vibration that was derived using a vibration controller was generated by using the following equations[10] so that they have the same PSD as the Gaussian random vibration that is derived using an actual vehicle.

$$a(t) = \sum_{k=1}^{n} A(k)\cos(2\pi k\Delta f t + \varphi(k)) \tag{2}$$

$$A(k) = \sqrt{2\Delta f S(k\Delta f)} \tag{3}$$

Here t is the time, n is the number of data items, Δf is the frequency resolution, $\varphi(k)$ $(k = 1, 2, \ldots, n)$ is the phase, and $S(k\Delta f)$ $(k = 1, 2, \ldots, n)$ is the PSD. The parameters that need to be defined in Equations (2) and (3) are $\varphi(k)$ and $S(k\Delta f)$. These were respectively set as uniform random numbers that range from 0 to 2π and the same PSD as "Vibration 3", generating the Gaussian random vibrations. The generated vibration in this way is used as the Gaussian random vibration that was derived using the vibration controller.

Figs. 7 and 8 depict the Gaussian random vibrations that are derived using an actual vehicle ("Vibration 3" is shown in Fig. 6) and a vibration controller, respectively. Meanwhile, Figs. 9 and 10 depict the PSDs and PDFs of the Gaussian random vibrations that are derived using an actual vehicle (Fig. 7) and a vibration controller (Fig. 8), respectively. It can be observed that both types of vibrations have almost the same PSD and PDF.

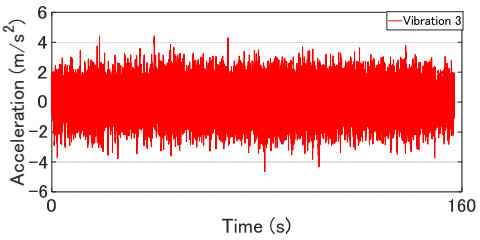

Fig. 7 Gaussian random vibration that is derived using an actual vehicle

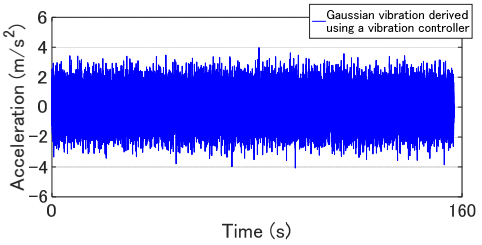

Fig. 8 Gaussian random vibration that is derived using a vibration controller

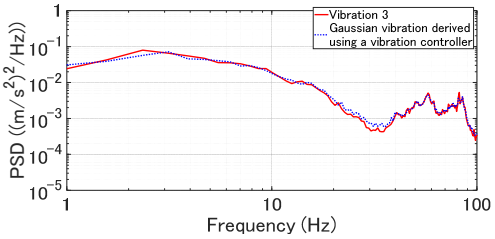

Fig. 9 PSDs of the Gaussian random vibrations that are derived using an actual vehicle and a vibration controller

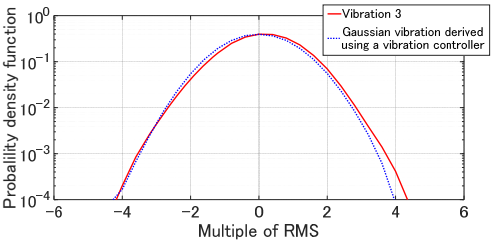

Fig. 10 PDFs of the Gaussian random vibrations that are derived using an actual vehicle and a vibration controller

3 Computational verification for equivalence of two types of Gaussian random vibration

3.1 Kurtosis response spectrum analysis[16)]

To verify the equivalence between the Gaussian random vibrations that are derived using an actual vehicle and a vibration controller, a kurtosis response spectrum analysis was conducted for both types of vibrations. Here, a kurtosis response spectrum is a plot of the kurtosis of the acceleration response to the base acceleration input for a series of SDOF systems. This spectrum is a similar concept to a shock response spectrum[17)] and an RMS response spectrum[18)] representing the maximum response and the RMS response of an SDOF system subjected to a certain waveform, respectively.

Fig. 11 illustrates a conceptual diagram of the kurtosis response spectrum. The horizontal axis represents the natural frequency of the SDOF system, whereas the vertical axis represents the response kurtosis that is obtained for each natural frequency. The procedure for obtaining a kurtosis response spectrum subjected to a certain acceleration waveform is described below.

1. Define the damping ratio ζ or the Q value ($Q \fallingdotseq 1/2\zeta$) of the SDOF system.
2. Define the natural frequency f_i of the SDOF system.
3. Calculate the response kurtosis K_i from the response acceleration $\ddot{x}_i$ of the SDOF system subjected to a certain acceleration waveform $\ddot{z}$.
4. Plot the defined natural frequency and the calculated response kurtosis on a graph.
5. Repeat the above procedure for other natural frequencies and connect the plotted points.

In kurtosis response spectrum analysis, the response kurtosis of a series of SDOF systems subjected to a certain acceleration waveform is obtained to determine whether the response kurtosis is amplified in a certain natural frequency bandwidth or not.

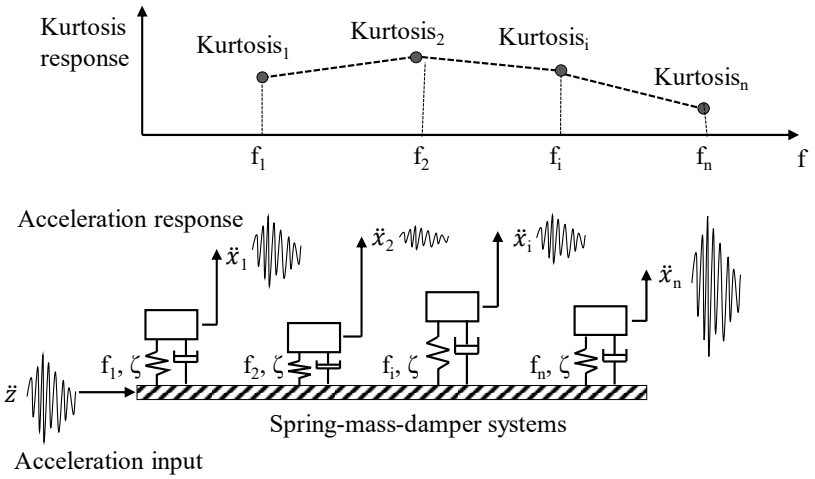

Fig. 11 Kurtosis response spectrum concept

3.2 Detailed procedure for calculation of kurtosis response spectrum

As depicted in Fig. 12, the cushioning material is assumed to be placed at the four corners of the packaged product. The product and the cushioning material are modeled as a rigid body and a spring-damper element, respectively. In this SDOF system, the motion of the product can be expressed as

$$m\ddot{x} + c\dot{u} + ku = 0 \tag{4}$$

where x is the absolute displacement of the product, $u = x - z$ is the relative displacement, z is the

absolute displacement of the vibration table, m is the rigid mass, k is the spring constant, and c is the damping coefficient. Substituting $\ddot{x} = \ddot{u} + \ddot{z}$ into Equation (4) yields

$$m\ddot{u} + c\dot{u} + \mathrm{ku} = -\mathrm{m}\ddot{z} \tag{5}$$

The spring constant k and the damping coefficient c can be expressed as

$$k = m{\omega_0}^2 \tag{6}$$

$$c = 2m\zeta\omega_0 \tag{7}$$

where f_0 is the natural frequency of the packaged product, $\omega_0 = 2\pi f_0$ is the natural angular frequency, and ζ is the damping ratio. Substituting Equations (6) and (7) into Equation (5) gives

$$\ddot{u} + 2\zeta(2\pi f_0)\dot{u} + (2\pi f_0)^2 u = -\ddot{z} \tag{8}$$

The parameters that need to be defined in Equation (8) are the natural frequency f_0, the damping ratio ζ, and the input acceleration $\ddot{z}$.

Since this study aims to obtain the kurtosis response spectrum of the Gaussian random vibrations that are derived using an actual vehicle and a vibration controller, the input acceleration $\ddot{\boldsymbol{z}}$ was set using the "Vibration 3" (Fig. 7) and the Gaussian random vibrations that are derived using a vibration controller (Fig. 8). The natural frequency was assumed to be within the range of 5–100 Hz and it was set to 5, 6 ..., and 100 Hz with intervals of 1 Hz. A plastic foam cushioning material was assumed to be used as the cushioning material, and the damping ratio ζ of the packaged product was set to 0.15 based on the damping ratios (0.06–0.29) that were investigated in a previous study. [19)]

The natural frequency f_0, the damping ratio ζ, and the input acceleration $\ddot{z}$ were set in this way, and the response acceleration $\ddot{u}$ and its kurtosis were calculated using the Newmark β method, which is a numerical integration method to solve differential equations. In the Newmark β method, the value of β was set as 1⁄4, which is an unconditionally stable value regardless of the time interval of the numerical integration. In addition, the time interval Δt was set as 1/20 ms, which is sufficiently small with respect to the measurement sampling frequency of 1280 Hz since Δt in the numerical integration is accompanied by a phase delay when the value is large.

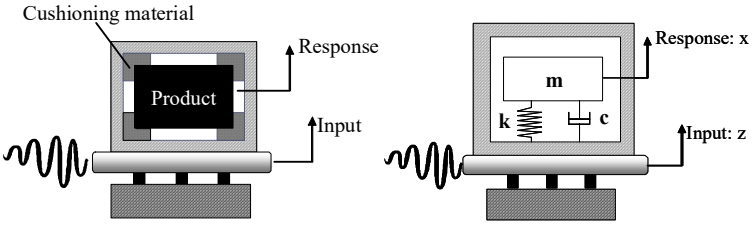

Fig. 12 Analytical model of a packaged product

3.3 Results

Fig. 13 compares the kurtosis response spectrum of the Gaussian random vibrations that are derived using an actual vehicle and a vibration controller. It can be observed that the response kurtosis of the Gaussian random vibrations that are derived using an actual vehicle varies with the natural frequency. For example, the maximum and minimum response kurtosis of the Gaussian random vibrations are close to four at a frequency of approximately 14 Hz and three at a frequency of approximately 70 Hz, respectively. In contrast, the response kurtosis of the Gaussian random vibrations that are derived using a vibration controller is always constant at approximately three regardless of the frequency. Even though the Gaussian random vibrations that are derived using an actual vehicle and a vibration controller almost have the same PSDs and PDFs, the kurtosis of the SDOF responses may vary with the natural frequencies of the packaged product.

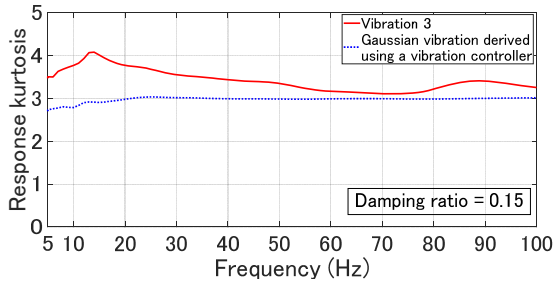

Fig. 13 Kurtosis response spectrum of the Gaussian random vibrations that are derived using an actual vehicle and a vibration controller

3.4 Discussion

We further compared the SDOF response to two types of vibrations with natural frequencies of 14 Hz and 70 Hz.

Figs. 14 and 15 depict the SDOF responses (natural frequency = 14 Hz and damping ratio = 0.15) to two types of Gaussian random vibrations that are derived using an actual vehicle and a vibration controller, respectively. Figs. 16 and 17 depict the corresponding PSDs and PDFs, respectively. It can be noted that the SDOF responses to the two types of vibrations exhibit the same PSDs but they have different PDFs. The PDF of the SDOF response to the Gaussian random vibrations that are derived using a vibration controller remains Gaussian, whereas the SDOF response to the Gaussian random vibrations that are derived using an actual vehicle varies from Gaussian to non-Gaussian. Figs. 18 and 19 depict the SDOF responses (natural frequency = 70 Hz and damping ratio = 0.15) to the two types of vibrations, respectively. Figs. 20 and 21 depict the corresponding PSDs and PDFs, respectively. It can be further noted that the SDOF responses for the two types of vibrations exhibit the same PSDs and PDFs. In general, as depicted in Fig. 21, when the vibrations that are derived using an actual vehicle follows the Gaussian distribution, the SDOF response also has a Gaussian distribution. However, as depicted in Fig. 17, even if the vibrations that are derived using an actual vehicle follows the Gaussian distribution, the SDOF response does not necessarily follow the Gaussian distribution. In other words, the PDF of the SDOF response may be different, even for vibrations that have the same PSD and PDF. Therefore, to accurately replicate the vibration environment, it is necessary to consider the PSD and PDF, as well as the PDF of the SDOF response.

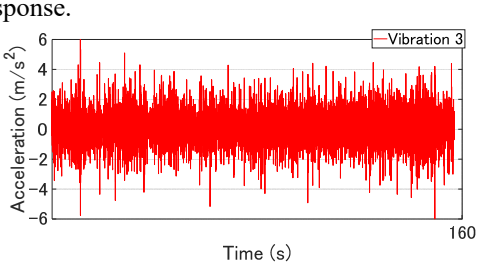

Fig. 14 SDOF response to the Gaussian random vibrations that are derived using an actual vehicle; natural frequency = 14 Hz, damping ratio = 0.15

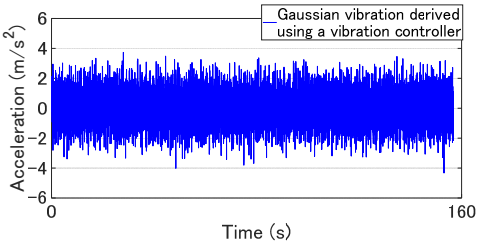

Fig. 15 SDOF response to the Gaussian random vibrations that are derived using a vibration controller; natural frequency = 14 Hz, damping ratio = 0.15

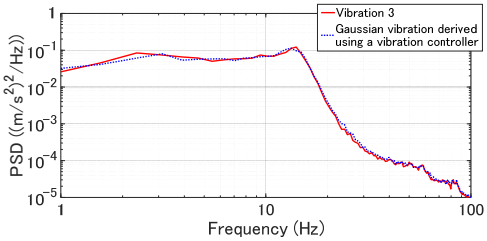

Fig. 16 PSDs of the SDOF response to the Gaussian random vibrations that are derived using an actual vehicle and a vibration controller; natural frequency = 14 Hz, damping ratio = 0.15

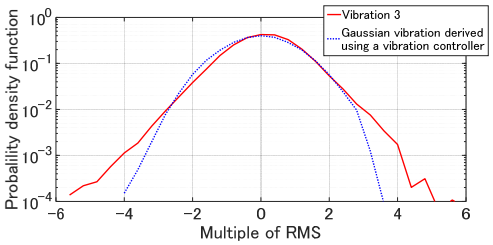

Fig. 17 PDFs of the SDOF response to the Gaussian random vibrations that are derived using an actual vehicle and a vibration controller; natural frequency = 14 Hz, damping ratio = 0.15

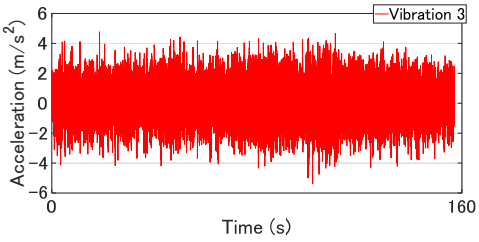

Fig. 18 SDOF response to the Gaussian random vibrations that are derived using an actual vehicle; natural frequency = 70 Hz, damping ratio = 0.15

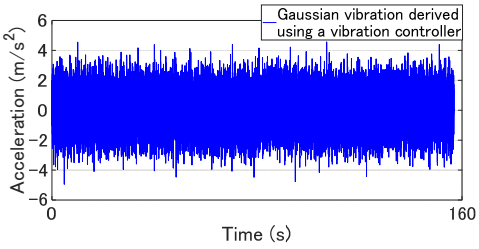

Fig. 19 SDOF response to the Gaussian random vibrations that are derived using a vibration controller; natural frequency = 70 Hz, damping ratio = 0.15

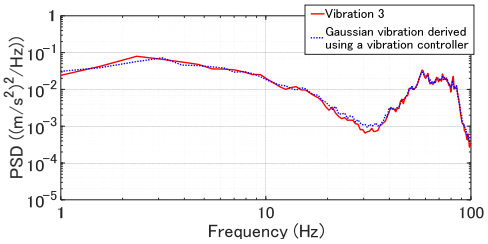

Fig. 20 PSDs of the SDOF response to the Gaussian random vibrations that are derived using an actual vehicle and a vibration controller; natural frequency = 70 Hz, damping ratio = 0.15

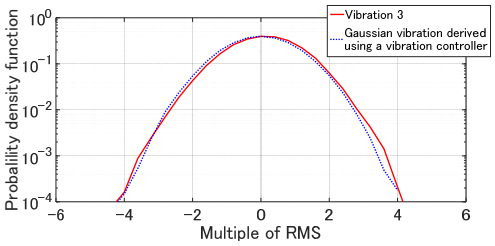

Fig. 21 PDFs of the SDOF response to the Gaussian random vibrations that are derived using an actual vehicle and a vibration controller; natural frequency = 70 Hz, damping ratio = 0.15

4 Vibration experiments

4.1 Method

In Chapter 3, the difference between two types of Gaussian random vibrations that are derived using an actual vehicle and a vibration controller was clarified by numerical analysis. It was indicated that the response kurtosis of the Gaussian random vibrations that are derived using a vibration controller is always approximately three regardless of the natural frequency, while the response kurtosis of the Gaussian random vibrations that are derived using an actual vehicle exceeds three depending on the natural frequency. It is not common that the response kurtosis of the Gaussian random vibrations exceeds three depending on the

natural frequency. In this chapter, to experimentally verify that the SDOF response of Vibration 3, which is the Gaussian random vibrations, may not be Gaussian depending on the natural frequency, vibration experiments are conducted. The experimental setup and the procedure are described below.

Polyethylene foam corner pads (SUNTEC FOAM™, expansion ratio: 45 times, Asahi Kasei Chemicals Corporation, Japan) were placed at the corners of an acrylic box (11.4 kg), as shown in Figs. 22 and 23. The acrylic box with the foam corner pads was placed in a corrugated fiberboard box to complete the dummy packaged product. Six types of corner pads with different bearing areas (Fig. 24) and two types of weights were prepared.

The vibration experiments were conducted under the conditions listed in Table 6. The dummy packaged product was fixed on top of a vibration table (Fig. 25), and the vibration table was vibrated vertically using the Gaussian vehicle vibrations shown in Fig. 7. An acceleration sensor was installed at the center of the acrylic box and the vibration table (Figs. 26 and 27), and the vertical acceleration of the acrylic box and vibration table was measured using a transport environment recorder tough logger (TR-1000, IMV Corporation, Japan), as shown in Fig. 28. The PSD was calculated from the measured acceleration, and the vibration transmissibility of the dummy packaged product was determined using the following equation:

$$H_{experiment}(f) = \sqrt{\frac{P_{response}(f)}{P_{input}(f)}} \tag{9}$$

where $H_{experiment}(f)$ is the vibration transmissibility obtained in the experiment, and $P_{response}(f)$ and $P_{input}(f)$ are the PSDs of the acrylic box and the vibration table, respectively.

The vibration transmissibility of the modeled packaged product (Fig. 12) can be expressed as equation (10) and is defined as a function of natural frequency f_0 and damping ratio ζ.

$$H_{theory}(f) = \sqrt{\frac{1+(2\zeta(\frac{f}{f_0}))^2}{\sqrt{\left(1-(\frac{f}{f_0})^2\right)^2+(2\zeta(\frac{f}{f_0}))^2}}} \tag{10}$$

Here, f_0 and ζ were determined as the natural frequency and damping ratio, respectively, that minimize the sum of squared errors between $H_{theory}(f)$ and $H_{experiment}(f)$ via the non-linear optimization method using the GRG solver built in Microsoft Excel 2016.

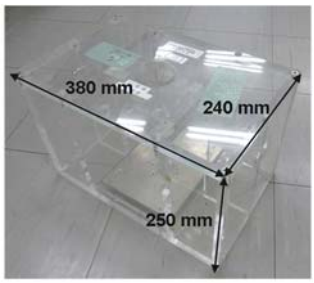

Fig. 22 Acrylic bcx

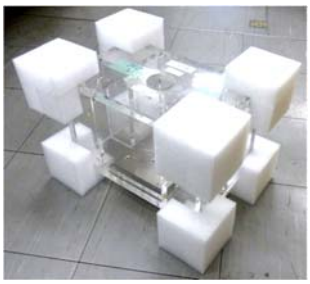

Fig. 23 Layout of the cushion corner pads

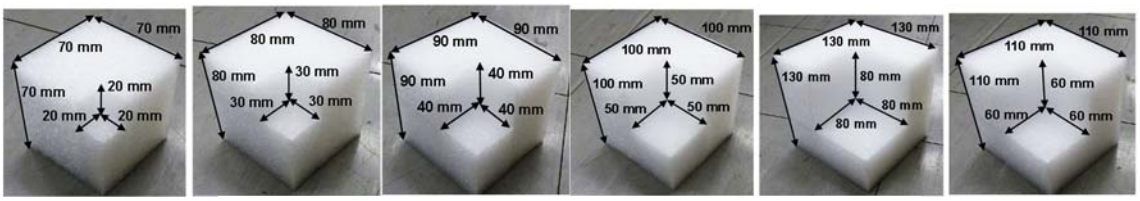

Fig. 24 Dimensions of the cushion corner pads

Table 6 Experimental conditions

Status	Cushion bearing area (mm)	Product weight (kg)	Static load (MPa)
Condition 1	20 × 20	22.9	0.14
Condition 2	20 × 20	17.1	0.10
Condition 3	20 × 20	11.4	0.070
Condition 4	30 × 30	11.4	0.031
Condition 5	40 × 40	11.4	0.017
Condition 6	50 × 50	11.4	0.011
Condition 7	60 × 60	11.4	0.0078
Condition 8	80 × 80	11.4	0.0044

Fig. 25 Dummy packaged produ
fixed on top of the vibration tab

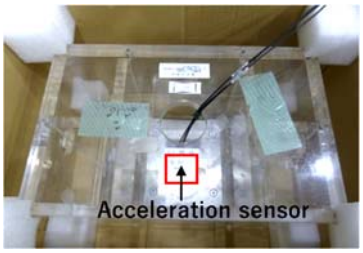

Fig. 26 Acceleration sensor installed on the acrylic box

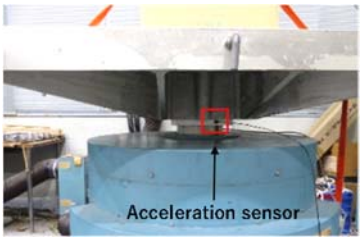

Fig. 27 Acceleration sensor installed on the vibration table

Fig. 28 Transport environment recorder tough logger (TR-1000, IMV Corporation, Japan)

4.2 Results

Fig. 29 shows the acceleration data measured on the vibration table and acrylic box. Fig. 30 shows the vibration transmissibility obtained from the vibration experiments and the vibration transmissibility determined by the least squares approximation. Table 7 summarizes the natural frequency and damping ratio determined by the least squares approximation, and the kurtosis and RMS of the acceleration data measured on the vibration table and acrylic box. Fig. 31 shows the plot for the kurtosis values measured on the acrylic box, using data summarized in Table 7 and shown in Fig. 13.

As shown in Table 7 and Fig. 31, at the natural frequencies of 15.2 Hz or 19.1 Hz, the response kurtosis is close to 4, which is much higher than 3. On the other hand, at the natural frequencies of 37.9 Hz or 43.6 Hz, the response kurtosis is close to 3. Thus, the experimental data are in good agreement with the results of the kurtosis response spectrum analysis; further, the SDOF response of the Gaussian random vibration may become a non-Gaussian random vibration, depending on the natural frequency of the packaged product.

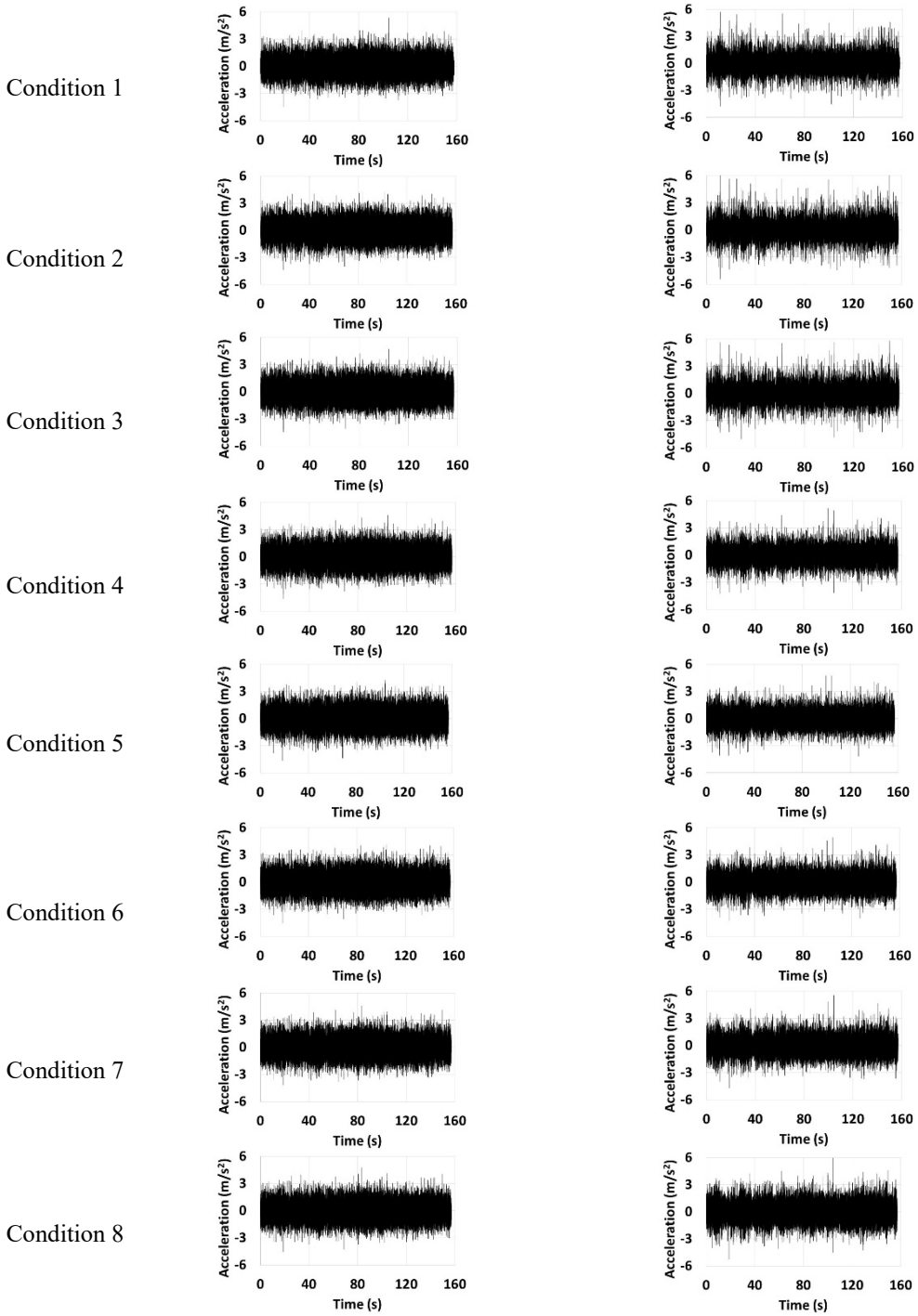

(a) Vibration table (b) Acrylic box

Fig. 29 Acceleration data measured on the vibration table and on the acrylic box for each experimental condition

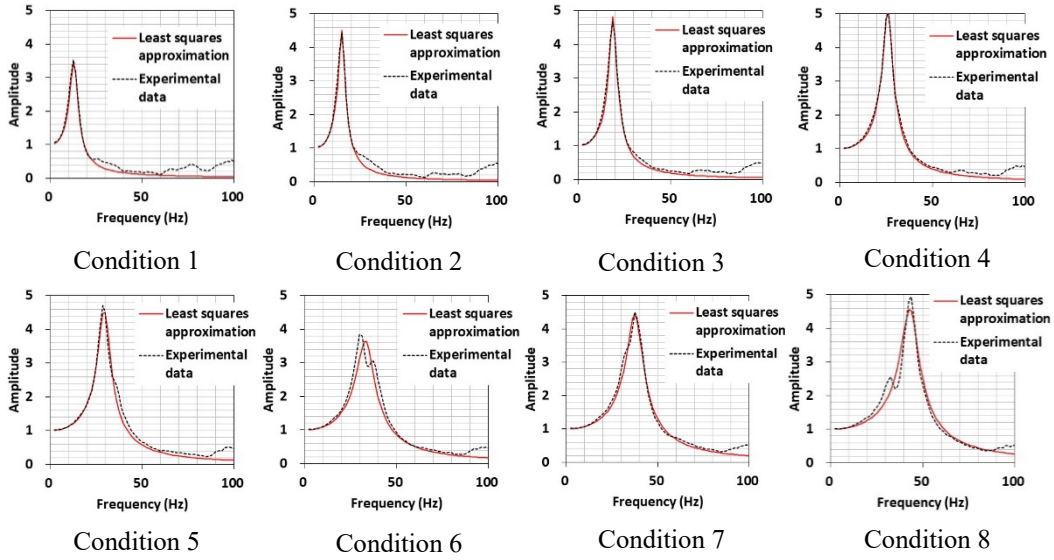

Fig. 30 Vibration transmissibility curves for each experimental condition

Table 7 Natural frequency and damping ratio of the packaged product, and the kurtosis and RMS of the acceleration data measured on the vibration table and acrylic box

	Natural frequency (Hz)	Damping ratio	Kurtosis (Vibration table)	RMS (m/s^2) (Vibration table)	Kurtosis (Acrylic box)	RMS (m/s^2) (Acrylic box)
Condition 1	13.2	0.15	3.13	0.87	3.61	1.03
Condition 2	15.2	0.11	3.13	0.88	3.94	1.07
Condition 3	19.1	0.11	3.12	0.89	3.87	1.02
Condition 4	26.2	0.10	3.11	0.89	3.57	0.88
Condition 5	29.8	0.11	3.15	0.89	3.48	0.86
Condition 6	33.8	0.14	3.12	0.89	3.40	0.87
Condition 7	37.9	0.12	3.13	0.89	3.34	0.90
Condition 8	43.6	0.11	3.14	0.89	3.30	0.96

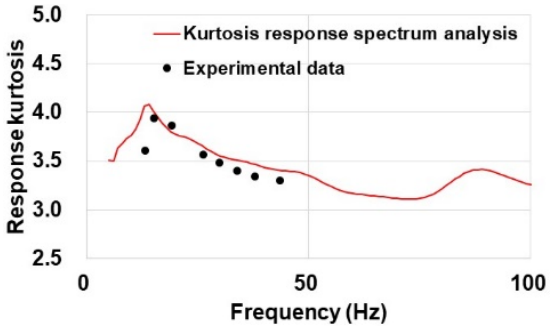

Fig. 31 Kurtosis response spectrum for different natural frequencies with the experimental data

4.3 Discussion

Furthermore, we zoomed into the section where the difference in the SDOF response was remarkable under each condition, particularly the section from 10 s to 12 s, and we examined the factors that caused the SDOF response of Gaussian random vibration to be non-Gaussian. Fig. 32 shows the zoomed-in figure of the section from 10 s to 12 s in Fig. 29. The acceleration data measured on the vibration table were almost the same shape in each experiment, and the input acceleration was the same. In contrast, the response acceleration on the acrylic box indicates that the vibration surrounded by the dotted line considerably differs depending on the experimental conditions. In particular, for conditions 1-3, the vibration surrounded by the dotted line is greatly amplified, and the response vibration becomes large. On the contrary, for conditions 4-8, no large amplification is observed. Thus, “Vibration 3” includes the vibration components that trigger amplification, which causes the SDOF response of the Gaussian random vibration to be non-Gaussian.

In this experiment, the vibration table was vibrated vertically and the vertical acceleration of the acrylic box was measured. In reality, the lateral acceleration is also considered to occur, but in this experiment, polyethylene foam corner pads were placed at the corners of an acrylic box, so significant vibration was not observed in the horizontal direction. Therefore, it is considered that the vertical vibration was dominant, and the dispersion of energy to other than the vertical direction was small.

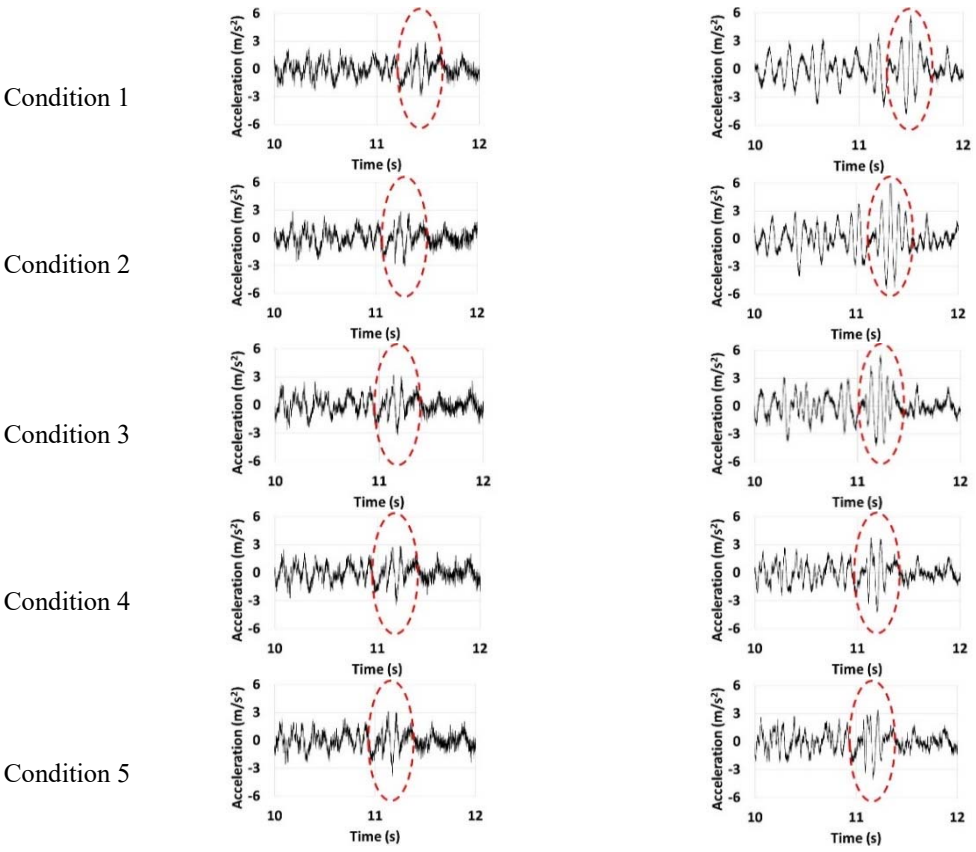

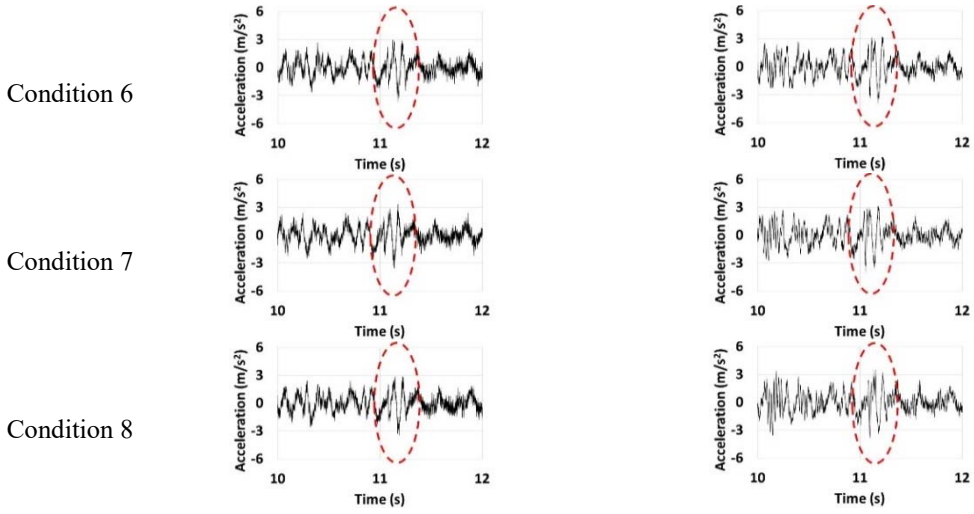

(a) Vibration table (b) Acrylic box

Fig. 32 Zoomed-in figure of the section from 10 s to 12 s in Fig. 29

5 Conclusion

In this study, a kurtosis response spectrum analysis was conducted for the Gaussian random vibrations that are derived using an actual vehicle and a vibration controller, and the equivalence between these two types of vibrations was verified. The findings of this study are summarized as follows:

1. The response kurtosis of the Gaussian random vibrations that are derived using a vibration controller is close to three regardless of the natural frequency. Meanwhile, the Gaussian random vibrations that are derived using an actual vehicle may be greater than three depending on the natural frequency.
2. Solely the PSD and PDF are not sufficient to completely understand the nature of the vibration, and the PDFs of the SDOF responses need to be considered.
3. The kurtosis response spectrum is effective as an index to visualize the difference between the Gaussian random vibrations that are derived using an actual vehicle and a vibration controller.

References

1) JIS Z 0200:2020, Packaging - Complete, filled transport packages - General rules for the compilation of performance test schedules.
2) ISO 4180:2019, Packaging - Complete, filled transport packages - General rules for the compilation of performance test schedules.
3) ASTM D4169-16, Standard Practice for Performance Testing of Shipping Containers and Systems.
4) Rouillard, V. and Sek, M.A. Monitoring and simulating non-stationary vibrations for package optimization. Packag Technol Sci., 13, 149-156 (2000)
5) Alexander Steinwolf, W.H. Connon III. Limitations of the Fourier transform for describing test course profiles. Sound and vibration, February, 12-17 (2005)
6) Lepine, J., Rouillard, V., and Sek, M. Review Paper on Road Vehicle Vibration Simulation for Packaging Testing Purposes. Packag Technol Sci., 28, 672- 682 (2015)
7) Steven R. Winterstein. Nonlinear Vibration Models for Extremes and Fatigue. Journal of Engineering Mechanics, ASCE, 114, 1772-1790 (1988)

8) David O. Smallwood. Generating Non-Gaussian Vibration for Testing Purposes. Sound and vibration, October, 18-24 (2005)
9) Alexander Steinwolf. Closed-loop shaker simulation of non-Gaussian random vibrations; Part 2 Numerical and experimental results. Test Engineering and Management, 68, 14-19 (2006)
10) Steinwolf A, Ibrahim RA. Numerical and experimental studies of linear systems subjected to non-Gaussian random excitation. Probabilist Eng Mech., 14, 289-299 (1999)
11) Hosoyama A, Saito K, Nakajima T. Non-Gaussian random vibrations using kurtosis. In Eighteenth IAPRI World Packaging Conference, DEStech Publications, Inc.: San Louis Obispo (CA), USA, 2012.
12) Rouillard V, Sek MA. Synthesizing nonstationary, non‐Gaussian random vibrations. Packag Technol Sci., 23, 423-439 (2010)
13) Griffiths KR, Hicks BJ, Keogh PS, Shires D. Wavelet analysis to decompose a vibration simulation signal to improve pre-distribution testing of packaging. Mechanical Systems and Signal Processing, 76-77, 780-795 (2016)
14) Zhou, H., and Wang, Z. W. A New Approach for Road‐Vehicle Vibration Simulation. Packag Technol Sci., 31, 246-260 (2018)
15) Bonnin AS, Nolot JB, Huart V, Pellot J, Krajka N, Odof S, Erre D. Decomposition of the acceleration levels distribution of a road transport into a sum of weighted Gaussians: Application to vibration tests. Packag Technol Sci., 31, 511-522 (2018)
16) Hosoyama, A, Tsuda, K, Horiguchi, S. Development and validation of kurtosis response spectrum analysis for antivibration packaging design taking into consideration kurtosis. Packag Technol Sci., 33, 51– 64 (2020)
17) Irvine T. An introduction to the shock response spectrum. Rev P Vibrationdata, 1-73 (2012)
18) Irvine T. An Introduction to the Vibration Response Spectrum. Rev D Vibrationdata, 1-20 (2009)
19) Kazuaki KAWAGUCHI, Study on equivalence of simulated drop test for packaged freight, PhD thesis, Kobe University

Acknowledgements

This work was partially supported by JSPS KAKENHI grant number JP18K13964.

(Received 1March 2021)
(Accepted 8June 2021)

車両振動から得られるガウス型ランダム振動の一自由度系応答の非ガウス性

細山　亮、津田　和城、堀口　翔伍

本研究の目的は、実輸送から抽出されたガウス型ランダム振動と現状の振動制御器で再現したガウス型ランダム振動の等価性を検証することである。本研究では、包装品を一自由度系システムと想定し、これら 2 種類のガウス型ランダム振動に対する一自由度系応答から尖度を求めることで、両者の等価性について評価を行った。その結果、現状の振動制御器で再現したガウス型ランダム振動ではその一自由度系応答もガウス型ランダム振動となるのに対し、実輸送から得られたガウス型ランダム振動ではその一自由度系応答は、包装品の固有振動数によって、非ガウス型ランダム振動となることが明らかとなった。本研究結果は、振動台でのパワースペクトル密度と確率密度分布だけでは、完全にその振動の性質を把握することができず、その一自由度系応答の確率密度分布についても考慮する必要があることを示唆している。

キーワード：ランダム振動、ガウス分布、一自由度系、振動試験、尖度応答スペクトル